

White-light-induced drift in cylindrical and spherical geometries

V. G. Arkhipkin, D. G. Korsukov, and A. K. Popov

Institute of Physics and Krasnoyarsk University, 660036 Krasnoyarsk, U. S. S. R.

A. M. Shalagin

Institute of Automation and Electrometry, 630090 Novosibirsk, U. S. S. R.

A. D. Streater

Department of Physics, Building 16, Lehigh University, Bethlehem, Pennsylvania 18015

(Received 18 December 1989)

White-light-induced drift is a process whereby white light can separate species in a gas mixture. The effectiveness of the process is determined by the competition between the increasing velocity selectivity of excitation and the loss of excitation as the propagating light is absorbed and reemitted. We show that the divergence of real light sources affects this competition and find conditions relating source dimensions and densities for which the white-light-induced drift effect should be strong. Geometries with cylindrical and spherical symmetries are considered.

INTRODUCTION

It has been suggested that light-induced drift (LID) may account for some puzzling astrophysical phenomena, including anomalous abundances in chemically peculiar stars and the distribution of the isotopic hydrogen ratio $[H]/[D]$ in the solar system.^{1,2} Of particular importance is the fact that LID can cause the separation of components in a gas mixture even if the gas is irradiated by *white* light, i.e., by light with a flat spectral intensity distribution (white LID or WLID).³ The physics of this phenomenon consists of the following. As light propagates through a gas mixture containing two (or more) species with closely spaced transitions (e.g., a mixture of two isotopes of the same atomic species), dips are formed in the intensity spectrum due to absorption and re-emission at the resonant frequencies ("Fraunhofer lines"). Thus the intensity spectrum may be asymmetrical about the transition frequency of a species a_1 because of the absorption at the transition frequency of another species a_2 . Conversely, there is an asymmetry about the transition frequency of the species a_2 due to the absorption line of species a_1 . Due to the Doppler effect, the spectral asymmetry leads to a velocity asymmetry of excitation (i.e., to a stronger excitation in certain velocity classes). This, in turn, in the presence of a buffer gas, results in a flow (light-induced drift) of species a_1 and a_2 in opposite directions. The species with the lower transition frequency is pushed and the other species is pulled (provided the cross section for elastic collisions of the excited particles is larger than the cross section for the unexcited particles).

In a plane-wave geometry, WLID was studied in Ref. 3. However, most white-light sources (both natural and artificial) are divergent. The strength of the WLID effect

is determined by the competition of the increasing velocity selectivity of excitation as structure forms in the intensity spectrum with the decreasing excitation rate due to the loss of radiation intensity near resonance. By affecting this competition, the radiation divergence can significantly change the WLID process in natural objects and laboratory experiments. In this paper we shall study WLID for geometries in which the white-light source has a cylindrical or spherical shape, as shown Fig. 1.

EQUATIONS COUPLING THE TRANSPORT OF ATOMS AND LIGHT

First we consider cylindrical geometry. A cylinder-shaped lamp of radius r_0 is placed coaxially in a flask with an outer radius R . The space between the cylindri-

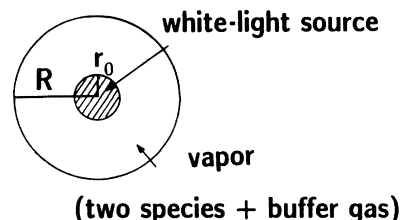


FIG. 1. White-light-induced separation of species in a gas mixture in spherical or cylindrical geometry. The white-light source, and the vapor containing two optically active species 1 and 2 in a much more abundant buffer gas, are shown. A thin layer of atoms on the inner surface maintains fixed densities N_{10} and N_{20} at r_0 .

cal surfaces filled with a mixture of two optically absorbing atomic species (e.g., an isotopic mixture of an element) and a much more abundant buffer gas. The radiation intensity is assumed to depend only on the distance from the light source. Under these assumptions and for weak fields, the variation of the steady-state atomic concentrations $N_i(r)$ (for $i = 1, 2$) at radius r is described by³

$$\frac{dN_1(r)}{dr} = \frac{v_{d1}}{D_1} N_1(r), \quad \frac{dN_2(r)}{dr} = \frac{v_{d2}}{D_2} N_2(r), \quad (1)$$

where

$$v_{di} = - \frac{v_{2i} - v_{1i}}{v_{1i}} \frac{B_i}{A_i + v_{2i}} \times \int d\omega I(\omega, r) \int dv \frac{v W_i(v) \Gamma_i / \pi}{(\omega - \omega_i - kv)^2 + \Gamma_i^2} \quad (2)$$

is the induced drift velocity; v_{2i} and v_{1i} are the elastic-collision frequencies of the excited and unexcited particles of species a_i with the buffer gas; D_i are the diffusion coefficients; B_i are the Einstein absorption coefficients; A_i are the Einstein spontaneous-emission rates; Γ_i are the homogeneous linewidths (half width at half maximum, including natural and pressure broadening under the impact approximation); $W_i(v)$ are the one-dimensional Maxwell velocity distributions; $I(\omega, r)$ is the radiation intensity; and $k = \omega/c$, where ω is the frequency and c is the speed of light.

It has also been assumed that the intensity is purely radial. Nonradial rays of the extended source may reduce the LID effect somewhat, especially near the inner wall. An intensity that is not purely radial could be taken into account by using an angle-dependent intensity and including an extra angular integration in Eq. (2).

The transport equation for light that is used in Ref. 3 is actually easier to work with under conditions of cylindrical symmetry than in the plane-wave case. With the above assumptions it will take the form

$$\frac{1}{r} \frac{\partial [rI(\omega, r)]}{\partial r} = - [\alpha_1(\omega, r) + \alpha_2(\omega, r)] I(\omega, r), \quad (3)$$

where $\alpha_i(\omega, r)$ are the weak-field absorption coefficients.

We have left out a term on the right-hand side of Eq. (3) corresponding to the reemission of light by the atoms. In Ref. 3 this term could be left out because the vapor cell geometry was long and narrow, allowing light re-emitted by the atoms to escape without being reabsorbed. For cylindrical and spherical cells the reradiated light does not readily escape. However, radiative transfer calculations that include reemission usually assume a spherically symmetrical radiation field for determining the atomic response. Under this assumption the reradiated light would not influence the drift velocity. In any case, if light coming directly from the source accounts for a significant fraction of the excitation (thus at moderate optical depths), the reemission term (the emission coefficient) will not have a large effect on the drift velocity and can be left out. For large optical depths, especially near the outside surface of the vapor, this approximation is not valid. It is interesting to note that light-induced drift should be sensitive to the directional asymmetry of the intensity spectrum, which is very difficult to determine for real systems of large optical depth.⁴

Equation (3) has the solution

$$I(\omega, r) = I_0 \frac{r_0}{r} \exp \left[- \left[\sigma_1 \frac{\phi_1(\omega)}{\phi_1(\omega_1)} \int_{r_0}^r dr' N_1(r') + \sigma_2 \frac{\phi_2(\omega)}{\phi_2(\omega_2)} \int_{r_0}^r dr' N_2(r') \right] \right], \quad (4)$$

where $\phi_i(\omega)$ are the Voigt line shapes and σ_i are the line-center optical cross sections. It is convenient to express Eqs. (1) and (2) in a reduced form,

$$\frac{dn_1}{d\xi} = a n_1(\xi) u_1(\xi), \quad \frac{dn_2}{d\xi} = a n_2(\xi) u_2(\xi),$$

where

$$u_i(\xi) = \int \left\{ 1 - \frac{\xi_0}{\xi} \exp \left[- \left[\varphi(x - x_1) \int_{\xi_0}^{\xi} d\xi' n_1(\xi') + \varphi(x - x_2) \int_{\xi_0}^{\xi} d\xi' n_2(\xi') \right] \right] \right\} \rho(x - x_i) dx \quad (5)$$

and

$$\rho(x) = \int dy \frac{y \exp(-y^2) (a_v / \pi^{3/2})}{(x - y)^2 + a_v^2},$$

where

$$a = \frac{l_{\text{abs}}}{l_{\text{LID}}}, \quad n_i = \frac{N_i}{N_{10}},$$

where l_{abs} is the absorption length at line center for species 1 at the inner boundary and l_{LID} is a characteristic length for light-induced drift,

$$l_{\text{abs}} = (\sigma N_{10})^{-1} \quad \text{and} \quad l_{\text{LID}} = \frac{D v_1 (A + v_2)}{\bar{v} (v_2 - v_1) B I_0},$$

where

$$\xi = \frac{r}{l_{\text{abs}}}, \quad \xi_0 = \frac{r_0}{l_{\text{abs}}}, \quad x = \frac{\omega - \omega_1}{k \bar{v}},$$

$$a_v = \frac{\Gamma}{k \bar{v}}, \quad \bar{v} = \left[\frac{k_B T}{2m} \right]^{1/2},$$

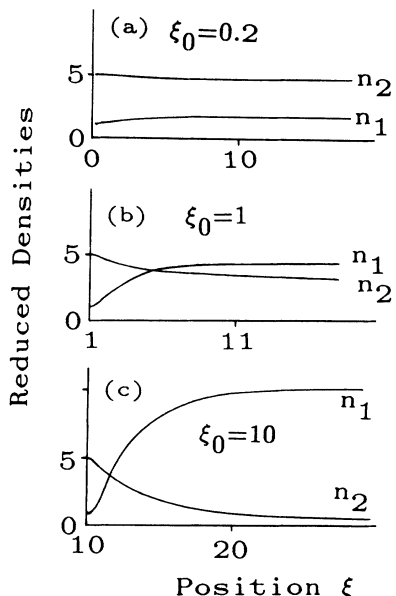


FIG. 2. The reduced densities n_1, n_2 as a function of reduced position ξ for the case of cylindrical waves. The numerical solutions are presented for atomic parameters $a=10$, $n_{20}=5$ ($n_{10}=1$ by definition), $x_2-x_1=2$, and $a_v=0.05$. Curves are shown for various values of the parameter $\xi_0=r_0/l_{\text{abs}}$.

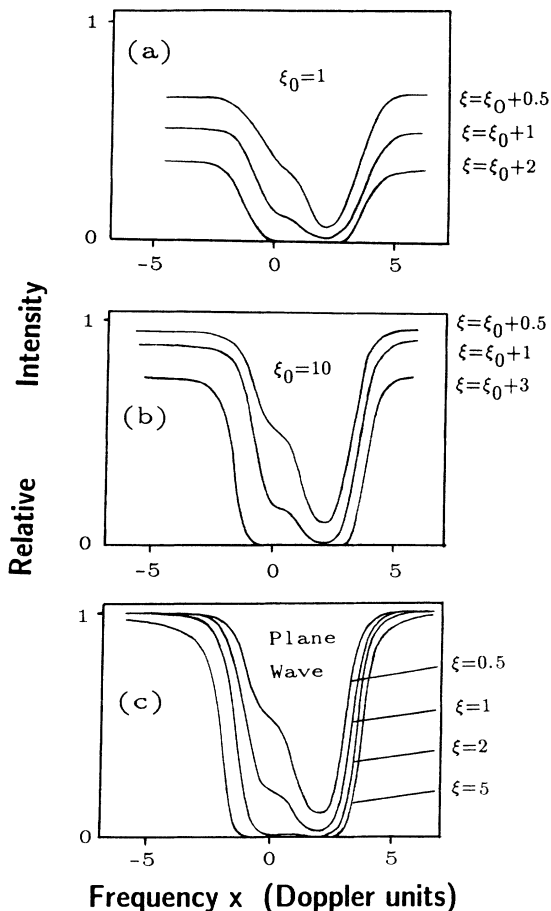


FIG. 3. Relative intensity spectra of light at various positions in the vapor for cylindrical waves with $\xi_0=1$ and $\xi_0=10$ and for the plane-wave case. Other parameters are the same as in Fig. 2.

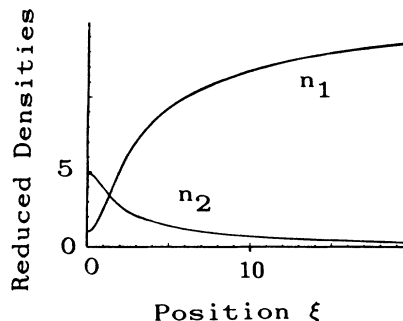


FIG. 4. The reduced densities n_1, n_2 as a function of reduced position ξ for the case of plane waves. Other parameters are the same as in Fig. 2.

where T is the temperature of the gas, k_B is the Boltzmann constant, and m is the atomic mass. The Voigt function $\varphi(x)$ is now normalized so that $\varphi(0)=1$. If the inner surface is coated with a transparent layer of the two species a_1 and a_2 , their densities are fixed at r_0 by their vapor pressures: $N_1(r_0)=N_{10}$ and $N_2(r_0)=N_{20}$. For simplicity we have now assumed that the atoms of both species are identical except for their resonant frequencies, and we have dropped the species subscripts on all other atomic parameters.

Spherical geometry is analyzed in a similar way, with the only difference being that in Eq. (4), which governs the intensity, the factor r/r_0 must be replaced by $(r/r_0)^2$ [and, consequently, ξ/ξ_0 by $(\xi/\xi_0)^2$ in Eq. (5)].

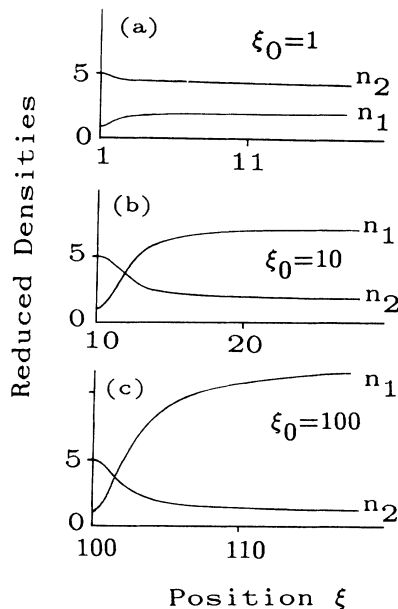


FIG. 5. The reduced densities n_1, n_2 as a function of reduced position ξ for the case of spherical waves. Results for various values of the parameter ξ_0 are shown. Other parameters are the same as in Fig. 2.

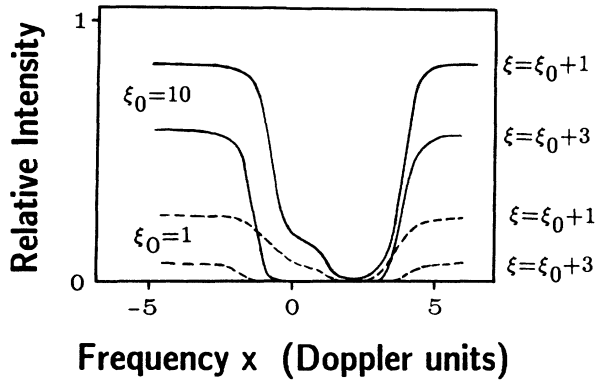


FIG. 6. Relative intensity spectra of light at various positions in the vapor for spherical waves with $\xi_0=1$ and $\xi_0=10$. Other parameters are the same as in Fig. 2.

NUMERICAL ANALYSIS

The intensity spectrum, and normalized concentrations n_1 and n_2 , have been numerically calculated for various values of the parameter ξ_0 . Note that ξ_0 can be changed experimentally either by changing the atomic density of species 1 or by changing the inner radius of the vapor cell. The results of cylindrical geometry are presented in Figs. 2 and 3. Calculations have been carried out for the atomic parameters $a=10$, $a_v=0.05$, $x_2-x_1=2$, $n_{10}=1$ (by definition $n_{i0}=N_{i0}/N_{10}$), and $n_{20}=5$.

Figure 3 shows the radiation spectrum (in arbitrary units) for various values of ξ_0 . For comparison, a similar radiation spectrum taken from Ref. 3 is shown in Fig. 3(c), which was calculated in the plane-wave case for the same atomic parameters. A comparison of Figs. 3(a) and 3(b) with Fig. 3(c) reveals differences in the intensity spectra associated with the fact that in cylindrical geometry the decrease in intensity occurs not only due to absorption but also due to radiation divergence (i.e., wave-front curvature). This difference is also manifest in the steady-

state densities. Figure 2 shows the densities for various values of ξ_0 , and Fig. 4 shows the densities for the plane-wave limit. A fairly effective separation of concentration occurs at $\xi_0=10$ [Fig. 2(c)], which is nearly the same as for the plane-wave limit (Fig. 4). Figures 5 and 6 show analogous results for spherical geometries. The calculations have been performed with the same parameters as in the cylindrical case. For a given ξ_0 , asymptotic separations are smaller than in the cylindrical case.

CONCLUSION

In cylindrical and spherical geometry the separation effect has been found to depend not only on the parameter $a=l_{\text{abs}}/l_{\text{LID}}$, but on $\xi_0=r_0/l_{\text{abs}}$ as well. For the case of cylindrical symmetry, an effective separation is expected if the absorption length is a few times smaller than the inner radius of the light source. This condition on the densities and source dimensions reduces the loss of intensity due to radiation divergence. For the parameters used here, the separation is largely established at a depth of about five absorption lengths into the vapor. This characteristic length is found to be essentially independent of the parameter ξ_0 .

For spherical geometry the effect of radiation divergence is more pronounced, as can be seen by comparing Figs. 2 and 3 with Figs. 5 and 6. This is because the intensity decreases faster with distance than for cylindrical geometry.

The results reported here are directly applicable to laboratory experiments. Astrophysical situations, however, are often more complicated. In stars, for example, the spectral lines are formed by repeated absorption and redistribution of light (radiative transfer). If the spectral lines form over a distance comparable to the stellar radius, the geometry effects discussed here will be important (although the line formation mechanism is more complicated). If LID is found to be important in determining the structure of illuminated interstellar gases or protostars, geometry effects might also be important.

¹S. N. Atutov and A. M. Shalagin, *Pis'ma Astron. Zh.* **14**, 664 (1988).

²S. N. Atutov (private communication).

³A. K. Popov, A. M. Shalagin, A. D. Streater, and J. P. Woerd-

man, *Phys. Rev. A* **40**, 867 (1989).

⁴A. Streater, J. Cooper, and D. E. Rees, *Astrophys. J.* **335**, 503 (1988).